

Establishing topological definitions for astrophysical spin, DM and DE, using Einstein's field equations.

CJ Blackwood
Michigan Theoretical Dynamics Institute
10.02.2025
cjblackwood@mtdi.org

Abstract:

The Ricci tensor and the Ricci scalar curvature, in the Einstein field equations, provide scale and curvature limits to the stress momentum tensor as well as establishing a topological equivalency to the bounds associated with the Laws of Thermodynamics. Mathematically, Ricci flow, and the Ricci tensor, reduce regions of high curvature and expand regions of low curvature. Like the "gravity funnel" we associate with topological representations of General Relativity, (GR), Ricci flow forces the stress tensor, in the field equations, into higher and higher curvatures, limited by the speed of light and the probabilities we associate with measurements of mass. In this extension of our previous discussions, we investigate equating Ricci flow, to topological spin at all scales of Lorentz invariance. Using the topological value that we have established for the Hubble constant, we establish equivalencies to the Metric Tensor and Einstein's cosmological constant. We, then, use the field equations to establish topological spin equivalencies to the Schrodinger equation, the Stefan-Boltzmann equations, Schwarzschild limits at the horizon of a black hole, Eddington accretion boundaries and measurements of Baryonic Acoustic Oscillations (BAO) in the Cosmic Microwave Background. In our equivalency to the CMB, we demonstrate how topological spin potentials, associated with intrinsic global and local phase bifurcation, establish oscillation in the CMB. We establish an equivalency between Hopf-Turing bifurcation patterns and the development of a dipole moment. To our knowledge, this is the first application of Hopf-Turing patterns as model for the development of BAO in the CMB. In our final section, we demonstrate how the field equations, and a topological definition for spin, are all that is necessary to understand the early appearance SMBH, LRD, Globular Clusters, and Spirals in the early universe.

1.0-Introduction

In this discussion, on the topology of "Dark matter" (DM) and "Dark Energy" (DE), we return to the basic requirements of Einstein's field equations, to explain many of the observations of galactic formation in the early universe. Our particular focus is to demonstrate how topological equivalencies to the Ricci Tensor (RT), and Ricci flow (RF), can be used to describe the measurements we associate with Dark Matter (DM). This paper is structured to introduce some of Bill Thurston's concepts in topology to a non-mathematically oriented audience as well as, potentially, shining some "light" on the Field Equations for those familiar with GR. In *Section-1.1*, we discuss the equivalencies established by General, and Special, Relativity (GR), with particular focus on the various components of the field equations and their relation to the topological limits of a 3-sphere. In *Section-1.2*, We discuss how geometric completeness is related to spin invariance at all scales of Lorentz invariance. As examples, we establish equivalencies to Hubble constant, the Schwarzschild limits at the horizon of a black hole and the Schrodinger equations. We also establish the equivalency between geometric completeness, topological spin and the gravitational wave boundaries associated with an Einstein ring. In *Section 1.3*, we discuss intrinsic spin and the establishment of BAO (Baryonic Acoustic Oscillation), and a dipole moment, in the Cosmic Microwave Background (CMB). We review the model for Hopf spin bifurcation that we established in our last few papers and demonstrate how intrinsic topological spin, and phase bifurcation, establish BAO in hyperbolic plane of the CMB. An equivalency between topological spin and the Stefan-Boltzmann equations is established. We proceed to discuss the possibility of Hopf-Turing spin bifurcation patterns observable in the PLANCK measurements of BAO in the CMB. In *Section 1.4*, we finish our investigation using current observations of the, surprising, structure and complexity in the early universe, including the early appearance of SMBH and Little Red Dots (LRD). We focus on demonstrating the application of Ricci flow as an equivalency to measurements in many of the major surveys of galactic structure in the early universe. As a point of interest for the reader, and to assure them that I am not a robot, I am including some of my original notes regarding the application of the field equations towards the modeling of early galactic probabilities (*Figure 1*).

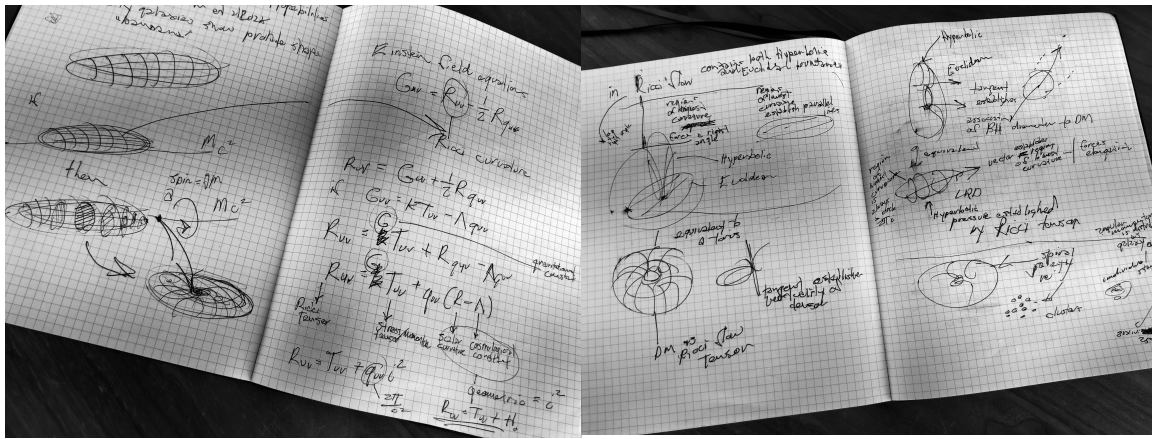


(Figure 1) Some of my early notes on the establishment of a topological definition at spin, at all scales of Lorentz invariance, using the tensors in Einstein's original field equations.

1.1-Using the field equations to set the topological boundaries for General Relativity, DM and DE

Einstein used an equivalency to acceleration to describe the “force” of gravity. He also demonstrated that every observer experiences this acceleration differently, based on their velocity and mass [1]. In this discussion we limit the equivalencies found in Einstein’s original field equations to the boundaries of geometric completeness established by Bill Thurston, on a 3-sphere [2]. If you are familiar with our previous work, defining the topological boundaries for DM, you know that we have been using the Hyperbolic and Euclidean planes to describe the relation between DM and gravity [8-14]. Gravity exists in the hyperbolic plane and DM, the tangential Euclidean plane. As Bill Thurston has proven, using the boundaries of completeness on a 3-sphere, hyperbolic and Euclidean coordinates have different rules concerning the measurements of lengths and angles and only the Euclidean plane can support parallel measurements. Hyperbolic space preserves angles, but not lengths. Unlike Euclidean space, hyperbolic space cannot admit parallel measurements (Figure 2).

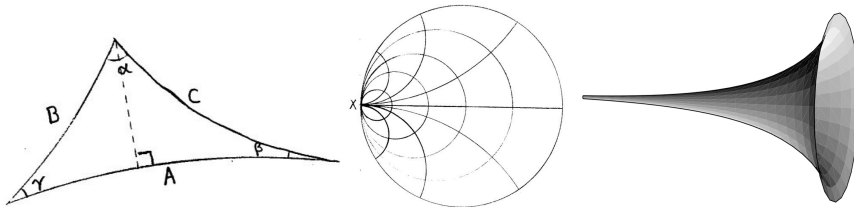


(Figure 2) Hyperbolic coordinates preserves angles, but not lengths. Thurston’s original drawings demonstrate that the Law of Sines and Fermat’s Theorem are both valid in hyperbolic space. In the center, a Thurston horosphere is illustrated using conformal closed curves. On the right, we include the 3-conformal surface tensor that can be equated to the stress tensor in Einstein’s field equations.

We are all familiar with representations of GR using a topological funnel. In the field equations, the vacuum of space is a smooth zero, represented by Einstein’s cosmological constant. In our topological equivalencies to GR, we will establish a zero point that is limited by the definition of geometric completeness on a 3-sphere. This allows us to establish a quantum zero point in the field equations, that is the inverse of our topological value for the Hubble constant. The advantages of a topological definition for the metric tensor, $\left(g_{\mu\nu} = \frac{c^2}{2\pi l^2}\right)$, the cosmological constant, $\left(\Lambda = \frac{2\pi l^2}{c^2} = H_0\right)$ and the Hubble constant will be demonstrated throughout this paper. However, before we proceed, it may be best to review the various components of the field equations and their functions. We ask the informed reader to, for the moment, excuse these gross generalizations of Einstein’s equations. Our goal with this paper is to demonstrate, to larger readership, the geometric nature of GR and 2-D topological manifolds. Clarity is our only goal for this discussion. The field equations can be stated as:

$$G_{\mu\nu} = R_{\mu\nu} - \frac{1}{2}Rg_{\mu\nu} \quad (1)$$

$$R_{\mu\nu} = GT_{\mu\nu} + g_{\mu\nu}(R - \Lambda) \quad (2)$$

Where, $(G_{\mu\nu})$ is the Einstein tensor, $(R_{\mu\nu})$ is the Ricci tensor, $(T_{\mu\nu})$ is the energy-stress-momentum tensor, (R) is the scalar curvature, (G) , the gravitational constant, $(g_{\mu\nu})$ is the metric tensor and (Λ) is Einstein's, infamous, cosmological constant. We intend to demonstrate that everything we need to set the quantum, and relative, definitions for DE, DM, and Astrophysical spin, is in the original field equations. Let's begin by discussing the tensors and their functions.

$(T_{\mu\nu})$ – The energy-stress-momentum tensor creates the equivalency to acceleration that Einstein used to describe gravity in terms of mass. The stress-momentum tensor can be equated to the boundaries of four-momentum on a 2-dimensional, topological manifold.

$(R_{\mu\nu})$ – The Ricci tensor modifies the stress momentum tensor based on the geometry of space-time. The Ricci tensor, and Ricci flow, maintains the constant positive curvature for all elements described in equation (2).

$(g_{\mu\nu})$ – The metric tensor is a geometric modifier to both the scalar curvature and the cosmological constant. The metric tensor allows us to define the relation between distance and angles in the hyperbolic plane of GR and the Euclidean plane of DM. In our discussion we will be using the inverse of our value for the, topological Hubble constant to define the actions of the metric tensor.

Like the, topological, boundaries of a 3-sphere, the Ricci tensor, in the field equations, forces a right angle between hyperbolic and Euclidean spaces and determines the relationship between lengths and angles. The Ricci tensor is a mathematical boundary for all curves related to scale. As scale gets smaller, the Ricci tensor and Ricci flow, force the topology of any manifold into higher curvatures. As we can see in Eq. (1) and (2), the metric tensor modifies the scalar curvature, (R) , and Einstein's vacuum constant, (Λ) and defines the lengths and angles in for all elements of the field equations. We will be using the inverse of our topological value for the Hubble constant to represent the actions of the metric tensor. This will allow us to substitute our, topological, value for the Hubble constant, $(\frac{2\pi i^2}{c^2})$, into the field equations as a scalable equivalency to the cosmological constant, without defining DE as a "force" or "particle".

$$H_0 = \frac{2\pi i^2}{c^2} = \Lambda \quad (3)$$

$$R_{\mu\nu} = GT_{\mu\nu} + g_{\mu\nu}(R - \frac{2\pi i^2}{c^2}) \quad (4)$$

$$R_{\mu\nu} = GT_{\mu\nu} + g_{\mu\nu}R - 1 \quad (5)$$

If the metric tensor is stated as the inverse of the vacuum value for the cosmological constant we get:

$$\text{if: } g_{\mu\nu} = \frac{c^2}{2\pi i^2} \quad (6)$$

$$\text{then: } R_{\mu\nu} = GT_{\mu\nu} + \frac{c^2}{2\pi i^2}R - 1 \quad (7)$$

$$R_{\mu\nu} - \frac{c^2}{2\pi i^2}R = GT_{\mu\nu} - 1 \quad (8)$$

$$R_{\mu\nu} + \frac{c^2}{2\pi i^2}R + 1 = GT_{\mu\nu} \quad (9)$$

Ricci flow, the Ricci metric tensor, and the Ricci scalar are defined by the same boundaries in the hyperbolic and Euclidean planes that we use to define the topological Hubble constant. Topological, boundaries for completeness in the, Euclidean, and hyperbolic planes is maintained by the Ricci scalar curvature (R) . The scalar

curvature is a topological metric that sets the scale of curvature of the Riemann manifold and the topological boundaries for Ricci flow in the hyperbolic and Euclidean planes. Unlike the tensors it modifies, the Ricci scalar curvature is integer based and can be used to describe quantum time boundaries.

$$\frac{2\pi i^2}{c^2} = \frac{\text{topological boundaries in the Euclidean plane}}{\text{measurements limited by the speed of light}} = \frac{\text{completeness in the Euclidean plane}}{\text{completeness in the hyperbolic, GR, plane}}$$

Completeness in the hyperbolic plane of GR is maintained by Ricci flow. In the Euclidean plane, geometric completeness results in the measurements we associate with DM. When we view measurements of the DM halo through a “lens” of geometric completeness, we can begin to see it as integral to GR and not in conflict with quantum mechanics. Because DM can be measured by its lensing equivalencies, strong gravitational lenses are the purest example of the observable validity of the field equations as a measurement of topological DM. Therefore, an Einstein ring equivalency is the most accurate measurement the effects of Euclidean DM in the hyperbolic plane of GR. In our papers, *Measuring the Universe Parts I, II (2023-24)*, we demonstrated an equivalency between the limits of geometric completeness and the limits of GR, represented by the boundaries of an Einstein ring, [11] (Figure 3).

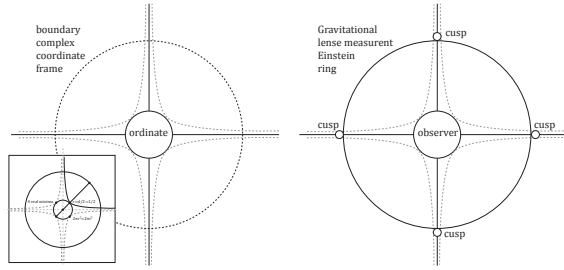


(Figure 3) Geometric completeness can be equated to the strong gravitational lensing measurements of an Einstein ring.

Geometric completeness in the hyperbolic plane can be equated to geometric completeness of the Ricci flow in the field equations. An Einstein ring equivalency allows us to tie topological spin directly to Ricci flow in the field equations. Because DM can be measured by its lensing equivalencies, an Einstein ring equivalency is the most accurate way we can measure the effects of Euclidean DM in the hyperbolic plane of GR. Our ring equivalencies, and topological value for spin, at all scales of Lorentz invariance, allow us to equate to all measurements associated with gravitational waves. In the next section we will demonstrate how we can use geometric completeness and the field equations, to set a common, and scale invariant, definition for quantum and astrophysical spin.

1.2-A scale-invariant definition of spin for quantum and relative measurements

In the current model of particle physics, spin is an intrinsic property of matter at the quantum scale. At quantum scales, spin is integer based. Fermions carry half integer spins, $(\frac{1}{2}, \frac{3}{2}, \frac{5}{2}, s = \frac{n}{2})$ and Bosons carry integer spins. It is important to remember that quantum spin is a reflection of the rules of probability and the Pauli exclusion principle. Particles are not actually spinning. In quantum physics, spin is a measurement of intrinsic angular momentum as a *probability* [3]. This is not the same as a “spinning” mass. Quantum probabilities are always held to the principle of uncertainty. A “spinning” mass is a continuous measurement of angular momentum that is not allowed under this principle. In order for GR to accommodate the probabilities associated with Fermi-Dirac and Bose-Einstein statistics it is important that they share a common definition of spin. *An astronomical definition of spin must be compatible with quantum probabilities in order conform to any definition of Lorentz invariance at all scales.* A topological definition of spin allows for us to equate quantum and relative measurements at all scales of probability. Because there is no such thing as a zero probability measurement, the limits of geometric completeness on a 3-sphere will allow us to equate topological spin to statistical completeness.

We can tie geometric completeness to the proof of the Poincare conjecture, produced by Gregory Perelman. Perelman used Ricci flow and the Ricci scalar to establish an equivalency to Riemannian geometric completeness [4]. His proof of the Poincare conjecture also proved the limits on a 3-sphere, established by Thurston. Equating topological spin to geometric completeness allows us to integrate statistical spin definitions into the field equations. Statistical spin is integer based, therefore, we must find a common component of the field equations that is limited to integers. Only one of the elements of the original field equations uses an integer-base. The Ricci scalar curvature is an integer-based metric that will allow us to equate to quantum, and statistical, spin to Ricci flow, in the field equations, using the topological limits of a 3-sphere:

$$R_{\mu\nu} + \frac{c^2}{2\pi i^2} R + 1 = GT_{\mu\nu} \quad (10)$$

$$\frac{c^2}{2\pi i^2} R = GT_{\mu\nu} - R_{\mu\nu} - 1 \quad (11)$$

$$H_0 = \frac{2\pi i^2}{c^2} = \frac{R}{(R_{\mu\nu} - GT_{\mu\nu} - 1)} \quad (12)$$

Because the Ricci scalar curvature is stated as an integer:

$$a_0 = 2\pi i^2 = \frac{nc^2}{(R_{\mu\nu} - GT_{\mu\nu} - 1)} \quad (13)$$

“Mass”, in both the hyperbolic and Euclidean planes, is defined by the Ricci scalar curvature modifying the tensors in the field equations. We can use our topological value for spin to establish a quantum zero point for measurements of mass in the hyperbolic plane of GR:

$$if: M_0 = \frac{n}{(R_{\mu\nu} - GT_{\mu\nu} - 1)} = \frac{\text{completeness in the Euclidean plane}}{\text{measurement in the hyperbolic plane}} \quad (14)$$

$$a_0 = 2\pi i^2 = (M_0)c^2 \quad (15)$$

We now have a definition of mass, (M_0), using Ricci flow, that that brings us back to Einstein's original; equivalency between energy and matter. We can demonstrate scale invariance by equating our value for topological spin to the Schwarzschild equations and the Schrodinger equations describing the quantum limits of the wave function. Schwarzschild limits are easily equated to our topological definition for intrinsic spin at the scale of a BH:

$$\frac{a_0}{c^2} = \frac{2\pi i^2}{c^2} = \frac{2GM}{c^2} = H_0 \quad (16)$$

At quantum scales, the topological spin-equivalencies we have established can be integrated into the Schrodinger wave equations [3]:

$$i\hbar \frac{\partial}{\partial t} |\psi(x, t)\rangle = \hat{H} |\psi\rangle \quad (17)$$

$$\overleftrightarrow{a}_0 = 2\pi i^2 = \frac{\overleftrightarrow{\lambda^2}}{n} \quad (18)$$

$$\overleftrightarrow{a}_0 = 2\pi i^2 = \frac{\overleftrightarrow{\lambda^2}}{n} = i\hbar \frac{\partial}{\partial t} |\psi(x, t)\rangle = \hat{H} |\psi\rangle \quad (19)$$

$$2\pi i^2 = \frac{i\hbar}{2\pi} \frac{\partial}{\partial t} |\psi(x, t)\rangle = \hat{H} |\psi\rangle \quad (20)$$

$$\frac{\overleftrightarrow{i}}{\hbar} = \frac{\partial}{\partial t} |\psi(x, t)\rangle = \hat{H} |\psi\rangle = 2\pi i^2 = \overleftrightarrow{a}_0 \quad (21)$$

$$\overleftrightarrow{a}_0 = 2\pi\overleftrightarrow{i}^2 = \frac{\overleftrightarrow{\lambda}^2}{n} = \frac{\overleftrightarrow{i}}{h} \quad (22)$$

Integrating our, topological, definition of spin into the Schrodinger equation allows us to describe relative and quantum wave probabilities at any scale. In the next section we will demonstrate how we can use our topological value for completeness, in the hyperbolic and Euclidean planes, to explain the establishment of a dipole moment and Baryonic Acoustic Oscillations (BAO) in the Cosmic Microwave Background (CMB).

1.3-Rici flow and Baryonic Acoustic Oscillations in the CMB

Bose-Einstein, Fermi-Dirac and Maxwell-Boltzmann statistics have very specific topological boundaries but share a universal scalability associated with rules of completeness. In the early universe, all three statistical variations work together as phase variations. As we have been discussing, a common definition of spin, at global local scales allows us to model hyperbolic GR and the Euclidean DM halo simultaneously. Because DM exists in the Euclidean plane, we can only measure its effects in momentum space. In our last few papers, we established the global, and local, nature of the statistical phase transitions at high redshifts. Global phase probabilities are Euclidean, like DM, and local phase probabilities, like the laws of Thermodynamics are tied to the speed of sound and matter wave potential in the hyperbolic plane [14]. Both global and local phases are driven by a common phase bifurcation transition. In our model of the early universe Hopf-bifurcation adds intrinsic spin to both quantum and relative measurements. We use a Hopf bifurcation transition between statistical phases to establish intrinsic spin at all scales of probability, (Figure 4).

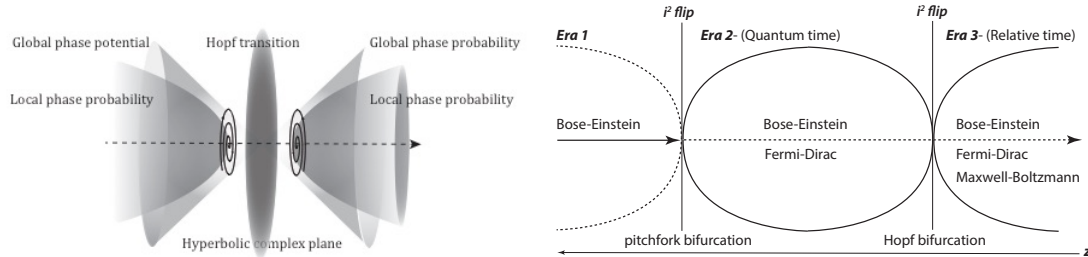


(Figure 4) Global and local phase probabilities are driven by the topological requirements for geometric completeness in both the hyperbolic plane of GR and the Euclidean halo of DM. Hopf-bifurcation complex transitions adds intrinsic spin to all scales of Lorentz invariance.

Hopf fibrations are well-known topological equivalents to the boundaries of a 3-sphere. Vectored Hopf fibrations, in hyperbolic space, can be equated to a torus in Euclidean space [5,6,7]. It is, perhaps, best to assume the reader is not familiar with the mathematics associated with Hopf fibrations. For this discussion, all we must remember is that every Hopf fiber or bundle can be reduced to a circle [5,6,7]. Therefore all Hopf transitions, or equivalencies to a 3-sphere, are valid under our proof of Geometric Completeness.

A compelling example of Hopf-Turing spin bifurcation at all scales, can be seen in the Planck measurements of Baryonic Acoustic Oscillations (BAO) in the Cosmic Microwave Background (CMB). The measurement of Baryonic Acoustic Oscillation in the early universe, and its growth through time, is a global phase probability in the hyperbolic plane. PLANCK, DESI and Sloan Digital Sky Survey measurements of BAO establish an intrinsic dipole moment in the CMB [15,16,17]

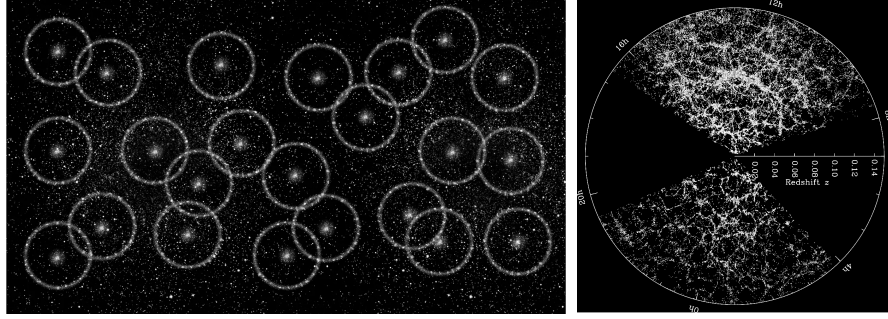


(Figure 5) The measurement of BAO in the CMB establishes the speed of sound based on the establishment of a dipole moment. On the left we show the establishment of BAO as a radius for the speed of sound. On the right we show how measurements of BAO scale across redshifts as measured by the Sloan Digital Sky Survey. Images: The Sloan Digital Sky Survey, The PLANCK Collaboration and The DESI Collaboration [ref 15,16,17]

The establishment of a dipole moment sets the speed of sound for all baryonic matter in the early universe. We can use the establishment of intrinsic topological spin to equate to these measurements. Vectored Hopf spin, in the complex plane, establishes the oscillation for all statistical potential in the hyperbolic plane [5,6,7]. We can equate Hopf spin oscillation, in the complex plane, to a global phase requirement for all BAO. Dipole measurements establish micro-fluctuations in temperature in CMB and follow Maxwell-Boltzmann statistical probabilities for a perfect blackbody. Inserting our topological value for spin into the Stefan-Boltzmann equations creates an equivalency to the laws of thermodynamics, and the establishment of a dipole moment in the CMB. The Stefan-Boltzmann equations equate energy and Luminosity to temperature [3]:

$$P = \epsilon \sigma A (T_o^4 - T_e^4) \quad (22)$$

$$P = \epsilon \sigma A (T_{eff})^4 \quad (23)$$

Where $P = \text{power}$, $\epsilon = \text{emmissivity} = 1$ (for an ideal blackbody), $A = \text{area}$, and $(T_o^4 - T_e^4) = (T_{eff})^4 = \text{effective temperature}$. Our value for topological spin can be substituted for (P) , to return us to the equivalencies to the field equations in the hyperbolic plane defined by thermodynamic probability:

$$\text{if: } M_0 = \frac{n}{(R_{\mu\nu} - GT_{\mu\nu} - 1)} \quad (24)$$

$$\text{and: } a_0 = 2\pi i^2 = (M_0)c^2 = P \quad (25)$$

$$P = \sigma A (T_{eff})^4 = (M_0)c^2 \quad (26)$$

$$(T_{eff})^4 = \frac{(M_0)c^2}{\sigma A} \quad (27)$$

$$(T_{eff})^4 = \frac{(M_0)c^2}{\sigma 4\pi r^2} \quad (28)$$

And if $r^2 = i^2$, then:

$$(T_{eff})^4 = \frac{(M_0)c^2}{\sigma 4\pi i^2} \quad (29)$$

$$(T_{eff})^4 = \frac{(M_0)c^2}{\sigma 2a_0} \quad (30)$$

$$(T_{eff})^4 \sigma = \frac{P}{2a_0} \quad (31)$$

$$a_0 = \frac{P_A}{2} \quad (32)$$

For all scale invariant spin, measured using the Stefan-Boltzmann equations:

$$a_0 = 2\pi i^2 = \frac{P_A}{2} = \text{Baryonic Acoustic Oscillation in the CMB} \quad (33)$$

Topological spin, at quantum scales, establishes the dipole moment an intrinsic spin of $\left(\frac{1}{2}\right)$ and (1) for all BAO.

We can use the same technique to establish topological equivalencies to Eddington accretion boundaries, between outward radiation pressure and the pull of gravity.

$$L = \frac{4GMc}{\kappa} = \frac{P_g}{P_r} \quad (34)$$

$$L = \frac{2a_0c}{\kappa} = \frac{P_g}{P_r} \quad (36)$$

Where $L = \text{luminosity}$, $(\kappa) = \text{opacity of the interstellar medium}$, $P_g = \text{gravitational potential}$, and $P_r = \text{outward radiation pressure}$. We can equate Eddington accretion boundaries to global and local phase probabilities by equating the opacity of the interstellar medium to local phase requirements in the hyperbolic plane. The opacity of the local interstellar medium, in the hyperbolic plane creates a local “reaction” to the global “diffusion”, of Euclidean phase probabilities:

$$\frac{2a_0c}{\kappa} = \frac{4\pi i^2 c}{\kappa} = 4\pi i^2 \left(\frac{\text{diffusion}}{\text{reaction}} \right) \quad (37)$$

The result, of the establishment of a dipole moment in the CMB, is the formation of a Hopf-Turing pattern between global spin diffusion and local spin reaction phases. We will assume the reader is somewhat familiar with Turing patterns, but not an expert. While Turing patterns are most often associated with patterns in Biology, the basis is geometric and stochastic. A simple way to think about Turing bifurcation is as an, equidistant, pattern forming on a 2-D surface because of a reaction-diffusion phase difference between two ideal fluids. When Hopf, complex, spin is added to a Turing pattern the result is a Hopf-Turing bifurcation, pattern, [5,6,7] (Figure 6).

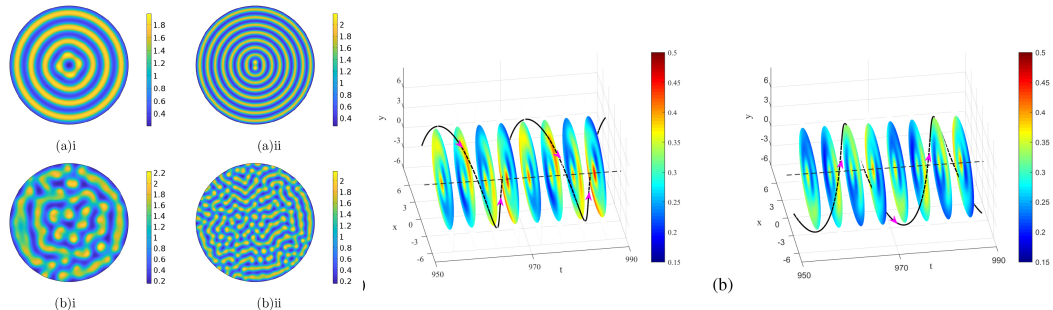


(Figure 6) Global and local phase probabilities are driven by the topological requirements for geometric completeness in both the hyperbolic plane of GR and the Euclidean halo of DM. The opacity of the local interstellar medium, in the hyperbolic plane creates a local “reaction” to the global “diffusion”, of Euclidean phase probabilities. The result is the formation of a Turing pattern. When Hopf, complex, spin is added to a Turing pattern the result is a Hopf-Turing bifurcation, pattern. (Images: Y. Chen, X. Zeng, B. Niu “Spatiotemporal patterns induced by Turing-Hopf interaction and symmetry on a disk” (2024)[ref 7]

Hopf-Turing bifurcation is scale invariant and is held the same boundaries, for completeness on a 3-sphere, that we have established in the field equations for our definition of topological spin. The difference between hyperbolic and Euclidean phase spin velocities forms the phase difference required for the formation of a HTB pattern. A Hopf transition is a topological transition through the imaginary plane. Because our definition of spin exists in the imaginary plane, we are able to use phase bifurcation to drive early galactic probabilities at global

and local scales. In fact, vectored Hopf-Turing bifurcation patterns growing on the surface of a sphere and torus present the same familiar pattern that we have come to associate with PLANCK measurements of the CMB (Figure 7).

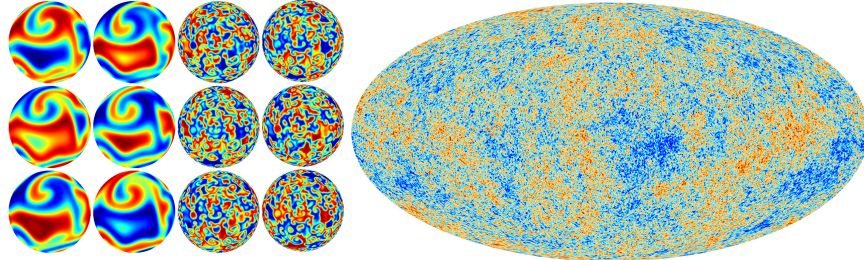


(Figure 7) Vectored Hopf-Turing bifurcation patterns growing on the surface of a sphere and torus present the same familiar pattern that we have come to associate with PLANCK measurements of the CMB. (Images: J Sánchez-Garduño, Krause, Castillo, Padilla "Turing-Hopf patterns on growing domains: The torus and the sphere" Journal of Theoretical Biology, Volume 481, (2019) and The PLANCK Collaboration) [ref 5,15]

Our equivalencies, to measurements of the CMB, are just another example of the flexibility of using a topological definition of spin that functions at all scales of Lorentz invariance. In our next section we will explore how Ricci flow, spin, and topological completeness determine probabilities for galactic formation in the early universe. As we have established, DM halos, for galaxies and clusters, are a Euclidean requirement for any vectored spin in the hyperbolic plane of GR. Topological spin transitions drive the global and local probabilities in the hyperbolic and Euclidean plane. It is intrinsic Hopf spin that drives the 4-momentum at astrophysical scales that we associate with DM measurements. A statistical frame of reference is scale invariant and is able to describe all aspects of quantum mechanics. In our final section, we will explore how topological spin and Hopf-Turing phase bifurcation drive the evolution of probabilities in the early universe at global and local scales.

1.4- Global and local phase evolution at astrophysical scales

We have established DM as a global phase probability in the Euclidean plane. Local measurements of GR are limited to the hyperbolic plane. In both planes, Bose-Einstein, Fermi-Dirac and Maxwell-Boltzmann statistics have very specific topological boundaries but share a universal scalability. In the early universe, all three statistical variations work together as global and local phase variations. Complicated structures, like SMBH, globular clusters, and spirals, at high red shift are all probabilities in conformal topological space. Bill Thurston reminds us, that, there as many homeographic knot equivalents as there are galaxies in the universe [2] (Figure 9).

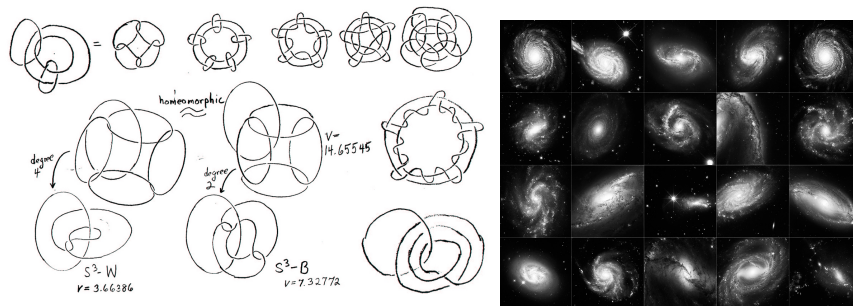


(Figure 9) There are as many homeographic knot equivalents as there are galaxies in the universe. Knots can combine to form larger structures like galactic clusters and the galactic web while still maintaining hyperbolic completeness. We show just a few examples of Thurston's drawings of knot equivalents next to a compilation of Hubble galaxy images.

Conformal topology of Ricci flow in the field equations, and a scale invariant definition of spin, is all we need to describe the early appearance of SMBH, "Little Red Dots" and fully developed spiral galaxies in the early

universe. We have established an equivalency between Lorentz invariant “mass” and the measurement of geometric completeness in the hyperbolic plane of GR:

$$M_0 = \frac{n}{(R_{\mu\nu} - GT_{\mu\nu} - 1)} = \frac{\text{completeness in the Euclidean plane}}{\text{measurement in the hyperbolic plane}} \quad (38)$$

$$a_0 = 2\pi i^2 = \frac{nc^2}{(R_{\mu\nu} - GT_{\mu\nu} - 1)} \quad (39)$$

$$a_0 = 2\pi i^2 = (M_0)c^2 \quad (40)$$

Our topological equivalency to Lorentz invariant mass allows us to cross the imaginary “boundary” between relative and quantum probability, at *all* scales of measurement. To model conformal topological probabilities, in the early universe, we establish a vector for spin in the hyperbolic plane of GR that acts as a local phase requirement. This can be thought of as an equivalency to Einstein’s cosmological constant, acting in opposition to our value for the topological Hubble constant. At high redshifts, the ratio between local hyperbolic, and global Euclidean, conformal spin topology establishes the geometric potential for LRD, globular clusters and dwarf galaxies (*Figure 8*).

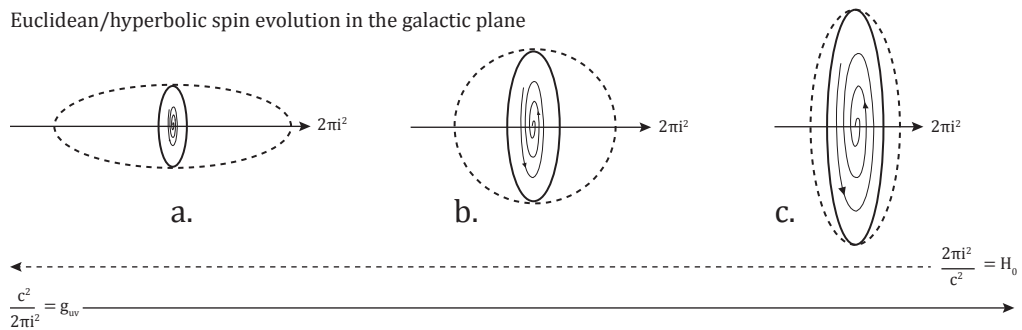


(Figure 8) Global and local phase probabilities are driven by the topological requirements for geometric completeness in both the hyperbolic plane of GR and the Euclidean halo of DM. (a.) Prolate spheroids have the highest ratio of Euclidean DM to hyperbolic GR as observed in LRD. (a.) The spherical geometry of globular clusters and star clusters is a result of a balance between hyperbolic and Euclidean conformal spin. (c.) In the local universe, the continuing expansion of hyperbolic spin flattens Euclidean DM to an oblate torus and the hyperbolic plane, into a Hopf spiral.

Prolate spheroids have the greatest Euclidean to hyperbolic ratio, representing the highest DM ratio. Prolate conformal topology can be seen in the extreme compaction of “Little Red Dots” (LRD) currently being observed at very high redshifts. Globular clusters, following spherical conformal topology, have the next highest ratio of Euclidean to hyperbolic spin. It is only in our own Era that we find a balance between hyperbolic and Euclidean spin topologies, resulting in the formation of spiral galaxies in conformal oblate geometry. Because topological spin is scale invariant, any of these geometries can exist at any redshift, however the scale may vary. A good example is the high intrinsic spin we see in dwarf galaxies. Dwarf galaxies show many of the traits of their much larger cousins, but contain a higher intrinsic spin because of the compaction of the conformal topological curves at smaller scales. The conformal topology of the early universe allows for the simultaneous development of complicated structures as distinct probabilities following the same local and global phase rules:

Super Massive Black Holes (SMBH)- In our paper describing a black hole as an ideal spin capacitor, we used Noether potential to describe spin [10]. The reason we did this is simple. Noether potential, and Noether current, are able to describe simultaneous real and imaginary states. Noether current carries three charge states positive, negative and, simultaneous, positive *and* negative. This apparent paradox is perfectly acceptable within the rules of quantum probability. The early appearance of quantum black holes as actual quantum “holes” allows us to equate the early appearance of SMBH to the knot topology of Bill Thurston. DM halos can be equated to a conformal torus in Euclidean space. The early appearance of SMBH, as complete quantum objects, is actually an expectation of this model and not a surprise development [15-23].

Little Red Dots (LRD)- LRD exhibit many indicators that they are driven by a central AGN in a compact pristine environment of gas. Observations of LRD show a characteristic broad emission line, indicative of very high velocity gas in the accretion disk of a BH. The prolate geometry exhibited by LRD indicate a very high DM/mass ratio. In terms of conformal topology, the curves are compressed in the hyperbolic plane of GR, which forces the increase in gas pressure feeding the SMBH. [19,20,23].

Globular clusters (GC) and star clusters (SC)- The, spherical, geometry of a cluster creates an equivalency between Euclidean and hyperbolic spin probabilities. Both galactic globular clusters and star clusters exhibit a central hyperbolic spherical geometry of GR that spins with the additional intrinsic spin in the Euclidean plane that we measure as DM. Although globular clusters and star clusters exist at, vastly, different scales, they exhibit the same conformal topology [15-23].

Spiral Galaxies (SG) and Barred Spiral Galaxies(BSG)- SG and BSG have the lowest Euclidean/hyperbolic ratios and are driven by the actions in the hyperbolic galactic plane. The central SMBH in these galaxies forces the topology of the spiral. SG and BSG exhibit the clearest observable example of Hopf intrinsic spin at all scale of probability. In spirals, local and global phase probabilities drive the conformal topology of the galactic plane. We recommend you read our last paper, "*Galaxies as probabilities*" (Blackwood, 2024), for a *complete* discussion of galactic probabilities driven by phase bifurcation [13].

Conclusions:

In this discussion, we have demonstrated an equivalency between Ricci flow in the field equations and the topological boundaries for geometric completeness established on a 3-sphere, by Bill Thurston. Using a topological value for spin, we demonstrated equivalencies to The Schrodinger equations, Schwarzschild's boundaries at the horizon of a BH, The Eddington equations, the Stefan-Boltzmann equations and Einstein's field equations. In addition, we believe we may be the first to apply Hopf-Turing boundaries to explain the establishment of BAO in the CMB. We discussed the probabilities associated with the appearance of SMBH, LRD, Globular Clusters and Spiral Galaxies, in the early universe and illustrated the evolution of intrinsic spin in the Euclidean and hyperbolic planes. The equivalencies we have established to the fundamental laws of physics, using the field equations, are what anyone should expect of a Lorentz invariant model that is scale invariant and able to describe all aspects of quantum and relative measurement. A common, topological, definition for spin can bridge the gap between GR and quantum probability, beautifully.

References:

(Note from author: My only reference for any Standard Model physics, as well as the probabilities associated with QED, is Richard Feynman's "Lectures on Physics" Vol. I-III. I also used Wolfram as a reference for some fundamental physics equations. For GR, my reference is the 15th Edition of Einstein's book on General and Special Relativity. Because the discoveries and understanding of LRD, Globular Clusters, and SMBH at high redshift is quite literally expanding on a daily basis. Therefore, for observational references, I have tried to stay with the major surveys as examples of some the, surprising, probabilities currently observed in the early universe. My contributions and images are all open access, however, the use of Bill Thurston's images was granted to the author for distribution to the scientific community, exclusively. All other uses are prohibited.)

- [1] **Einstein, Albert** "Relativity -The special and the General Theory " Random House, 15th edition (1961) Translation by Robert W. Lawson
- [2] **Thurston, William** "The geometry and topology of three-manifolds" American Mathematical Society (2022). Our use of Bill Thurston's images has been for distribution to the scientific community. All other uses are protected by the AMS copyrights and prohibited.
- [3] **Feynman, William** "Lectures on Physics" Vol. I-III Addison-Wesley Publishing (1965)
- [4] **Tao, Terry** "Perelman's proof of The Poincare Conjecture: A non-linier PDE perspective." arXiv:math/0610903v1
- [5] **Sánchez-Garduño, Krause, Castillo, Padilla** "Turing–Hopf patterns on growing domains: The torus and the sphere" *Journal of Theoretical Biology*, Volume 481, (2019)
- [6] **Van Gorder, R.A., Klika, V. & Krause, A.L.** "Turing conditions for pattern forming systems on evolving manifolds." *J. Math. Biol.* 82, 4 (2021)
- [7] **Y. Chen, X. Zeng, B. Niu** "Spatiotemporal patterns induced by Turing-Hopf interaction and symmetry on a disk" *Phys. Rev. E*, (Feb, 2024)
- [8] **Blackwood, CJ** "Time symmetry and measurement at the event horizon of a black hole." mtdi.org (Dec., 2018)
- [9] **Blackwood, CJ** "Establishing a minimum measurement boundary for the coupling of charged potentials eliminates the need for gluon fields." mtdi.org (Feb., 2019)
- [10] **Blackwood, CJ** "A black hole as an ideal spin capacitor" mtdi.org (Nov, 2019)
- [11] **Blackwood, CJ** "The Geometric Theorem of Completeness." Mtdi.org (Feb, 2021)
- [12] **Blackwood, CJ** "Measuring the Universe Pt. I- Dark Matter, Dark Energy, and The Big Flip." Mtdi.org (Jun, 2022)
- [13] **Blackwood, CJ** "Measuring the Universe Pt. II-Establishing the Topological Boundaries for Gravity, Dark Energy and Dark Matter in the early universe. " Mtdi.org (Dec, 2023)
- [14] **Blackwood, CJ** "Galaxies as probabilities." Mtdi.org (Dec, 2024)
- [15] **The Planck Collaboration** "Planck 2018 results. VI. Cosmological parameters" arXiv: 1807.06209v4 [astro-ph.CO] 9 Aug 2021
- [16] **Sloan Digital Sky Survey-V:** "Pioneering Panoptic Spectroscopy" arXiv: 250706989, (2025)
- [17] **DESI Collaboration** "DESI 2024 VI: Cosmological Constraints from the Measurements of Baryon Acoustic Oscillations" arXiv:2404.03002v2 [astro-ph.CO] 24 Apr 2024
- [18] **Freedman, Madore** "Status Report on the Chicago-Carnegie Hubble Program (CCHP): Three Independent Astrophysical Determinations of the Hubble Constant Using the James Webb Space Telescope" arXiv: 2408.06153v1 [astro-ph.CO] 12 Aug 2024
- [19] **Finkelstein et al**—"The Complete CEERS Early Universe Galaxy Sample: A Surprisingly Slow Evolution of the Space Density of Bright Galaxies at $z \sim 8.5-14.5$ " arXiv:2311.04279v1 [astro-ph.GA] 7 Nov 2023
- [20] **Viraj Pandya et al** "Galaxies Going Bananas: Inferring the 3D Geometry of High-redshift Galaxies with JWST-CEERS" 2024 *ApJ* 963 54
- [21] **D'Eugenio et al** "JADES and BlackTHUNDER: rest-frame Balmer-line absorption and the local environment in a Little Red Dot at $z = 5$ " arXiv:2506.14870
- [22] **Bingjie Wang et al** "UNCOVER: Illuminating the Early Universe—JWST/NIRSpec Confirmation of $z > 12$ Galaxies" 2023 *ApJL* 957 L34506.14870v1 [astro-ph.GA] 17 Jun 2025
- [23] **Maiolino et al** "JADES: comprehensive census of broad-line AGN from Reionization to Cosmic Noon revealed by JWST" arXiv:2504.03551v2 [astro-ph.GA] 29 Apr 2025
- [23] **Juodžbalis et al** "A direct black hole mass measurement in a Little Red Dot at the Epoch of Reionization" arXiv:2508.21748v1 [astro-ph.GA] 29 Aug 2025